Evaluation of organic matter characteristics of FO and RO concentrates

JunHee Ryu, Jaehyun Jung, YoungJae Yu, JiHyang Kweon*

Department of Environmental Engineering, Konkuk University, 120 Neungdong-ro, Gwangjin-gu, Seoul, Korea,
Tel. +82 2 454 4056; emails: carrot.jh@gmail.com (J. Ryu), jaehyun1122@naver.com (J. Jung), youngjae4355@gmail.com (Y. Yu),
Tel. +82 2 450 4053; email: jhkweon@konkuk.ac.kr (J. Kweon)

ABSTRACT

Numerous studies on forward osmosis (FO) have been conducted to understand fouling mechanisms better, especially compared to the reverse osmosis (RO) process. In this study, characteristics of concentrates from FO and RO filtrations were investigated to evaluate the rejection mechanisms of organic matter and to elucidate the effects of pressure on the active membrane side and hydrophobicity of organic compounds in the feed solution. The fluorescence excitation–emission matrix (FEEM) and a liquid chromatography-online carbon detector were employed to analyze the properties of organic matter. Secondary wastewater effluent was used to compare the concentrates. More humic-like fractions of organic matter remained in the concentrate from the FO than the RO process. In the concentrate from RO, building blocks and low-molecular weight acid were noticeable. The pressurized filtration experiments of the FO membrane revealed that operation with transmembrane pressure produced similar properties of the concentrates. In addition, Aldrich humic acid and sodium alginate were employed to determine the effects of hydrophobicity on the rejection of organic matter. The more hydrophobic organic matter, such as humic acid, showed greater concentration factors and higher intensity from FEEM analyses in the FO concentrates and a lower flux decline, as compared to the sodium alginate solution. Disposal strategies specific to FO concentrate and methods for anti-fouling should be further investigated based on the rejection properties of FO.

Keywords: Concentrate; Forward osmosis; Reverse osmosis; Dissolved organic matter; FEEM; LC-OCD

1. Introduction

The application of membrane filtration has substantially expanded due to its great separation efficiency and easy operation using automated systems. Recently, several novel technologies using forward osmosis (FO) membranes, including the recovery of high-salinity water from the oil/gas industry, resource recovery from wastewater, and zero liquid discharge systems, have been introduced [1]. Numerous studies on FO processes have also been conducted for the desalination of seawater. The FO process was first developed to enhance the overall performance of a

*Corresponding author.

reverse osmosis (RO)-based seawater desalination process through osmotic dilution [2–5]. FO is an osmotic-driven process that offers the advantage of low energy consumption as compared with pressure-driven processes such as RO and nanofiltration (NF) [6]. FO can also be applied as a pretreatment in the RO process, which can reduce energy consumption by increasing water production of the RO process.

An integrated FO-RO process has been considered to reduce the amount of effluent from wastewater facilities. In the FO-RO process, effluent from wastewater treatment plants (WWTP) is used as a feed solution and seawater is used as a draw solution. Across the FO membrane, purified water is pulled from the WWTP effluent to the seawater by an osmotic pressure difference between the feed and draw solutions. Therefore, the seawater is diluted and the WWTP effluent is concentrated.

There are obstacles, such as fouling and concentrate disposal, to overcome in membrane processes to accelerate their installation and use. The membrane process generates waste streams such as brine and concentrate that require special disposal methods to minimize their environmental impacts [7]. For instance, seawater and brackish water desalination plants affect the environment through their high-salinity wastewater discharges [8]. Water reclamation plants generate waste streams rich in salinity, nutrients, and pollutants.

The concentrates from the FO process in the integrated FO-RO system, therefore, require treatment prior to discharge to meet local or national water quality standards for discharge into rivers or anybody of receiving water. Treatment processes for FO concentrates are determined mainly based on characteristics of organic contents since the concentrates originate from wastewater effluent. Most studies on FO systems have focused on comparing the fouling phenomena of FO and RO systems [9]. Little research has been conducted on the characteristics of organic matter in FO concentrates. In particular, the rejection of FO membranes could differ from the rejection of RO membranes. Yangali-Quintanilla et al. [8] revealed that all anions and cations decreased, but dissolved organic carbon (DOC) slightly increased, in the diluted draw solution. The low-molecular weight (LMW) neutrals were suspected to pass through FO membranes although the nominal size of the neutrals was far greater than the rejected ions, suggesting different rejection mechanisms for FO and RO.

The FO-specific rejection would produce concentrates with distinctive water quality characteristics. Therefore, in this study, water quality characteristics of FO concentrate, mainly of organic matter, were explored to better understand which fractions of organics remained in concentrates and interacted with membrane surfaces. Secondary wastewater effluent (SWE) from a WWTP in operation was used as a feed solution for the FO process. The fluorescence intensity using the fluorescence excitation–emission matrix (FEEM) and the molecular weight (MW) distributions of DOC using size-exclusion chromatography (liquid chromatography-online carbon detector (LC-OCD)) were extensively used. In addition, the effects of hydrophobicity of the organic matter on water quality of FO concentrates were investigated using model water simulated synthesized with humic acid and sodium alginate.

2. Methods

2.1. Samples

2.1.1. Feed and draw solutions

Feed water was collected from SWE in operation at a WWTP in Guri-si, Gyeonggi-do, Korea. This feed water was the effluent from an anaerobic–anoxic–oxic (A^2/O) biological nutrient removal system. The SWE was refrigerated at 4°C until used. The FO experiments and water quality analyses were performed within two weeks. The characteristics of the SWE are outlined in Table 1. Since the water was treated to remove biological nutrients, concentrations of organic matter and inorganic nutrients were low. Feed solutions with approximately 60 mg/L of DOC were produced using humic acid (HA; Sigma-Aldrich, USA) to create a hydrophobic solution, and sodium alginate (SA; Junsei Chemical, Japan) to create a hydrophilic solution. HA, a typical hydrophobic organic matter, has a MW between 1.5 and 2.5 kDa. SA, a typical hydrophilic organic matter, has a MW between 12 and 80 kDa [10]. Each organic matter was dissolved in deionized (DI) water and filtered with a 0.45 μm membrane filter to create a stock solution (1 g/L). Each stock solution was mixed for 24 h to assure complete dissolution and was refrigerated at 4°C in a volumetric

Table 1
Water quality of the secondary wastewater effluent (SWE)

Parameter	Concentration
COD (mg/L)	22.09 ± 0.4
DOC (mg/L)	5.32 ± 0.1
T-N (mg/L)	17.70 ± 0.2
T-P (mg/L)	0.15 ± 0.01
UV_{254} (cm^{-1})	0.110
SUVA (L/m mg)	2.07

flask [11]. Draw solution was manufactured by dissolving sodium chloride (NaCl) to a concentration of 0.5 M, which has a similar conductivity to seawater.

2.2. FO and RO systems

Laboratory-scale cross-flow FO and RO modules were used to generate FO and RO concentrates. The FO module was built with dimensions of 110 mm long by 60 mm wide by 40 mm deep, whereas the RO module was smaller with dimensions of 85 mm long by 50 mm wide by 3 mm deep. Two low-pressure gear pumps (Cole-Parmer, Germany) were used to circulate the feed and draw solutions in the FO module. A high-pressure hydra-cell diaphragm pump (Wanner Engineering Inc., USA) was used to circulate the feed water in the RO module. The water flux of the FO experiments was calculated based on increases in the amount of the draw solution and that of the RO experiments was measured by collecting permeate in a beaker placed on an analytical balance (And, USA). The FO and RO experiments were operated at a recovery rate of 50%. The operational temperature for the FO and RO experiments was maintained at 20℃. During the RO experiment, a large amount of heat was produced by the high-pressure pump; thus, external cooling was performed using a laser chiller (Dolphin, Korea) to maintain a constant temperature.

2.3. Membranes

A thin film composite (TFC) polyamide FO membrane and a TFC polyamide RO membrane (RE8040-BE), both supplied by Toray Chemical (Korea), were employed in this study. The specifications of the two membranes are presented in Table 2. The membranes were distinguished as FOPA and ROPA by their originally intended uses. The FOPA membrane was operated in both the FO mode and RO mode. The same conditions used with the RO filtration, such as a transmembrane pressure of 20 bar and a cross-flow velocity of 15.7 cm/s, were applied during the RO mode

experiments using FOPA. The clean water flux (CWF) was measured for FOPA using the FO module and for ROPA with the RO module. For the measurement of the CWF of FOPA, DI water was used as a feed solution and 0.5 M NaCl was the draw solution in the FO module. The FOPA CWF of 26.8 Lm^{-2} h^{-1} in this study was lower than the expected flux supplied by the manufacturer, which could be obtained at the draw solution concentration of 1.0 M NaCl. For the measurement of the CWF of ROPA, DI water was used and the CWF was 52.1 Lm^{-2} h^{-1} at a transmembrane pressure of 8 bars. The CWF of ROPA was almost twice the CWF of FOPA.

2.4. Characteristics of organic matter

2.4.1. Fluorescence excitation–emission matrix (FEEM)

A FEEM spectrophotometer was used to establish the fluorescence intensity of dissolved organic matter (DOM). Fluorescence intensities were measured in a 1.0 cm quartz cell using FEEM (LS50B, Perkin Elmer, USA). FEEM was generated for each sample by scanning over excitation wavelengths between 220 and 400 nm at intervals of 10 nm and emission wavelengths between 280 and 600 nm at intervals of 2 nm. The DOM was characterized into four region peaks: tryptophan protein-like peak A (ex/em = 270–280/ 320–350 nm), aromatic protein-like peak B (ex/ em = 220–240/330–350 nm), humic-like peak C (ex/ em = 310–340/380–480 nm), and fulvic acid-like peak D (ex/em = 240–260/410–450 nm) [12].

2.4.2. Size-exclusion chromatography with LC-OCD

Size-exclusion chromatography (LC-OCD, DOC-Labor, Germany) was used to characterize the DOM with respect to MW. The LC-OCD was used to fractionate DOM into five fractions: biopolymers (such as polysaccharides, polypeptides, proteins, and amino sugars), humic substances (fulvic and humic acids), building blocks (hydrates of humics), LMW humic

Table 2
Specifications of FOPA and ROPA supplied from the manufacturer

	FOPA	ROPA
Material	Thin-film composite with polyamide coating	Thin-film composite with polyamide coating
Typical flux	35 Lm^{-2} h^{-1}	45 Lm^{-2} h^{-1}
	feed: DI, draw: 1M NaCl	Feed: 2,000 mg/L NaCl at 1,500 kPa
	20℃	25℃
Typical salt rejection	–	99.7%

substances, and LMW neutrals (such as alcohols, aldehydes, ketones, and amino acids) [13].

2.5. Analytical methods

The DOC concentration was determined by the combustion method using an organic carbon analyzer (TOC-V CPN, Shimadzu, Japan). UV absorbance (UVA) at 254 nm was measured using a UV–visible spectrophotometer (Genesys 10 UV, Thermo, USA). All samples were filtered with a 0.45 μm membrane filter (Whatman, GE, USA). The DOC and UVA amounts were used in the calculation of the specific UV absorbance (SUVA). The SUVA is calculated by dividing the UVA of the sample (cm^{-1}) by the DOC of the sample (mg/L) and then multiplying by 100 cm/m. SUVA is reported in units of L/mg m [14]. In addition, chemical oxygen demand (COD), total nitrogen, and total phosphate concentrations of the SWE were measured following the Standard Methods [14].

3. Results and discussion

3.1. Comparison of FO and RO concentrates of the SWE

3.1.1. Flux and water quality

The SWE was introduced to the FO and RO modules and the flux decline was monitored, as shown in Fig. 1. The flux decline by the RO filtration was more gradual than the flux decline by the FO filtration. Results by Lee et al. [11] also showed that RO flux decline was more severe than FO flux decline when the feed water contained either alginate or humic acid. However, the flux decline of RO was substantially high compared to the FO flux when bovine serum albumin (BSA) was used as feed water. Since the wastewater effluent presumably contained metabolic residues from micro-organisms, a majority of constituents could be similar to polysaccharide and alginate [11].
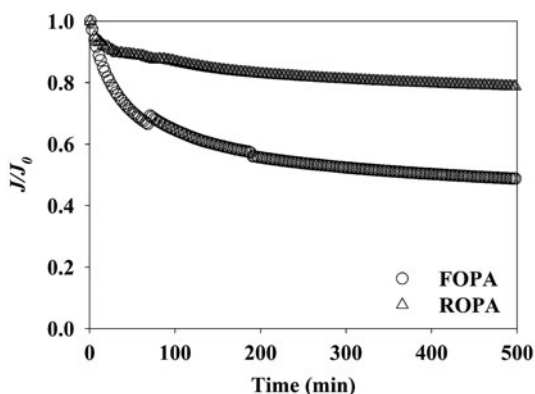
Table 3 illustrates the water quality characteristics of the FO and RO concentrates compared with the SWE. The FO and RO processes were both operated at the recovery rate of 50%. The rejection ratio of conductivity of RO in this experiment was 94.4%, which is similar to the specification of the membrane in Table 2. The FO used synthetic seawater with a conductivity of 48.2 ms/cm. The seawater was diluted to 35.26 ms/cm while the conductivity of the SWE was increased by concentration factors of three in the FO system. The water quality in terms of organic matter was evaluated using COD, DOC, UVA at 254 (UV_{254}), and SUVA. It appeared that the concentration factors of COD and DOC were in the range of 1.6–1.8, which was less than the calculated concentration factors, i.e. 1.993, based on the 94.4% rejection of the conductivity. In addition, the characteristics of concentrates from FOPA and ROPA were similar, except for the SUVA values. The high SUVA value of concentrates from FOPA indicated a high fraction of aromatic compounds as compared with that of concentrates from ROPA [15].

3.1.2. Fractionation of concentrate by FEEM

Fluorescence spectroscopy combined with excitation–emission matrix analysis (FEEM) has been widely used to characterize dissolved organic matter in water and wastewater [12]. The analyses of ratios of FEEM peak intensities were used to evaluate changes in organic matter in natural water systems as well as biologically degradable organic matter in WWTP effluents [16].

Fig. 2 illustrates typical fluorescence contour plots for bulk water (SWE), FO concentrate, and RO concentrate, respectively. It demonstrates the locations of the fluorescence intensity peaks A, B, C, and D. The *X*-axis and *Y*-axis represent the emission wavelength from 280 to 600 nm and the excitation wavelength from 220 to 400 nm, respectively. The contour lines represent the fluorescence intensity, which is the third dimension. One hundred contour lines are shown in each FEEM image.

Increased intensity of all fluorescence peaks was observed for the concentrates from the FO and RO filtration. Three main fluorescence intensity peaks were obtained for all samples. These identified peaks were observed at the following excitation and emission wavelengths: Tryptophan protein-like fluorescence (peak A) at 270–280 nm and 320–350 nm, respectively; aromatic protein-like fluorescence (peak B) at 220–240 nm and 330–350 nm, respectively; humic

Fig. 1. Flux of SWE during FO filtration with FOPA and RO filtration with ROPA.

Table 3
Water quality of the FO and RO concentrates

		COD (mg/L)	DOC (mg/L)	UV_{254} (cm^{-1})	SUVA (L/m mg)	Conductivity (ms/cm)
SWE		22.09 ± 0.4	5.32 ± 0.1	0.110	2.07	0.45
FO	Concentrate	37.01 ± 1.1	8.74 ± 0.1	0.191	2.19	1.39
	Diluted draw solution	–	–	0.022	–	35.26
RO	Concentrate	35.12 ± 1.3	9.80 ± 0.1	0.099	1.01	0.83
	Permeate	1.1 ± 0.7	0.65 ± 0.1	0.007	1.08	0.025
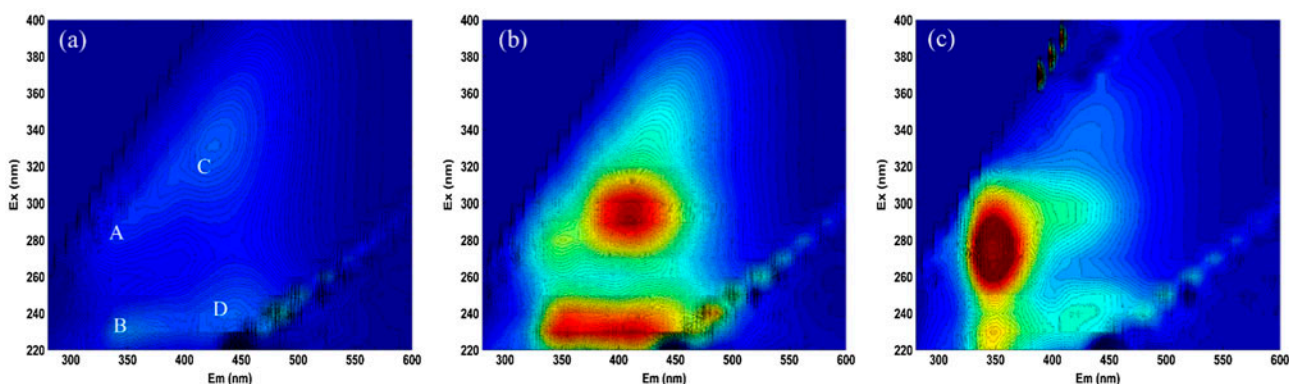
Fig. 2. FEEM images of: (a) SWE, (b) FO concentrate (FOPA), and (c) RO concentrate (ROPA); Peak (A): tryptophan protein-like (ex/em = 270–280/320–350 nm), Peak (B): aromatic protein-like (ex/em = 220–240/330–350 nm), Peak (C): humic acid-like (ex/em = 310–340/380–480 nm), and Peak (D): fulvic acid-like (ex/em = 240–260/410–450 nm).

acid-like (peak C) at 310–340 nm and 380–480 nm, respectively; and fulvic acid-like (peak D) at 240–260 nm and 410–450 nm, respectively [12]. The fluorescence intensity of bulk water (Fig. 2(a)) shows peaks B, C, and D. The concentrate from the RO filtration was dominated by the tryptophan protein-like peak A. The concentrates from the FO filtration were similar to the fluorescence intensity of the SWE but they demonstrated a greatly increased fluorescence intensity at humic acid-like peak C.

The organics remaining in the RO concentrates seemed to be extracellular biological organic matter fractions, which were extracted from activated sludge at the WWTP [12]. The organics deposited on the membrane surface during RO filtration were most likely highly interactive with the membrane surface under the conditions of the forced water flow to and pressure on the membrane surfaces. In contrast, the humic acid-like organic matter was noticeable in the remaining organic matter in FO concentrates.

3.1.3. Fractionation of concentrate by LC-OCD

Size-exclusion chromatography in combination with organic carbon detection (LC-OCD) was used to separate DOC into five fractions: Biopolymers, humic substances, building blocks, LMW neutrals, and acids. In the LC-OCD system, a size-exclusion column (HW-50S, Germany) is used to separate DOM. These fractions are quantified according to organic carbon concentrations using an organic carbon detector and characterized by a UV detector. Additional details regarding this system are provided elsewhere [17]. Fig. 3 shows the concentration distributions of DOC in the SWE and FO/RO concentrates. In agreement with the results obtained from fluorescence intensity, the concentrates from FO and RO filtrations showed higher concentrations for all fractions. However, the degree of increase was different for the two concentrates. Consistent with the FEEM intensities results, the FO concentrates showed far greater increases in humic substances and building block fractions, while the RO concentrates revealed substantial increases in building block and LMW acid fractions. The different fractions of organic components such as humic substances in RO concentrates and LMW acids and building blocks in FO concentrates indicated that the rejection mechanisms and fouling phenomena in FO filtration differed from those in RO filtration.
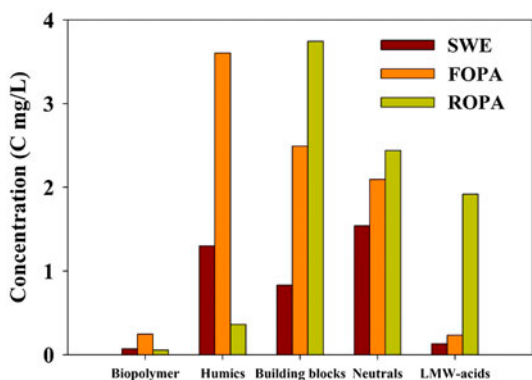
Fig. 3. Organic carbon concentrations with respect to biopolymers, humic substances, building blocks, neutrals, and LMW-acids using LC-OCD.

3.2. Organic matter in concentrates from pressure-driven filtration

3.2.1. Fractionation of concentrates by FEEM

To elucidate the differences in the rejection of the organic fractions from RO and FO filtration, the FOPA was installed in the RO module and operated at a transmembrane pressure of 20 bars and a recovery rate of 50%. The ROPA was also installed in the same condition. The feed water was the SWE. At the end of the filtration run, the concentrates were analyzed for organic fractions by FEEM. Fig. 4 shows fluorescence contour plots for the two concentrates from RO filtration. Surprisingly, the fluorescence intensity of the concentrates by FOPA and ROPA membranes were very similar. However, there was a great dissimilarity in concentrates from the FOPA membrane depending on the operational mode, either FO or RO. The

existence of extra loaded pressure on the membrane greatly influenced the characteristics of the concentrates and most likely the fouling behavior as well.

3.2.2. Flux and water quality

The flux decline patterns of experiments with FOPA and ROPA using the RO mode are shown in Fig. 5. The flux with ROPA was maintained at 95% of the initial flux, which was $50.94 \ Lm^{-2} \ h^{-1}$. The flux with FOPA showed a very rapid decline during the first 10 min of operation and then became stable between 70 and 80% of the initial flux. Since the initial flux of FOPA at the RO mode was high, i.e. $102.53 \ Lm^{-2} \ h^{-1}$ and the stable flux was approximately $80 \ Lm^{-2} \ h^{-1}$, the operation time to obtain 50% of the water recovery took only 5 h, which was shorter than the experiments with ROPA. The water permeation in the FO operation occurred by an osmotic pressure difference between 0.5 M NaCl and DI water, which was approximately 24 bar. Since the RO mode was operated at 20 bars of transmembrane pressure, the greater flux of FOPA in the RO mode did not result from driving force and was presumably due to structural properties, i.e. the very thin active layer in FO membranes [18]. In general, the FO membrane is not exposed to high pressure during typical operation, and thus the primary feature of the FO membrane is a very thin layer for water transport.

3.3. Effects of hydrophobicity on the fractionation of FO concentrates

Effects of hydrophobicity on characteristics of FO concentrates were investigated with HA and SA at
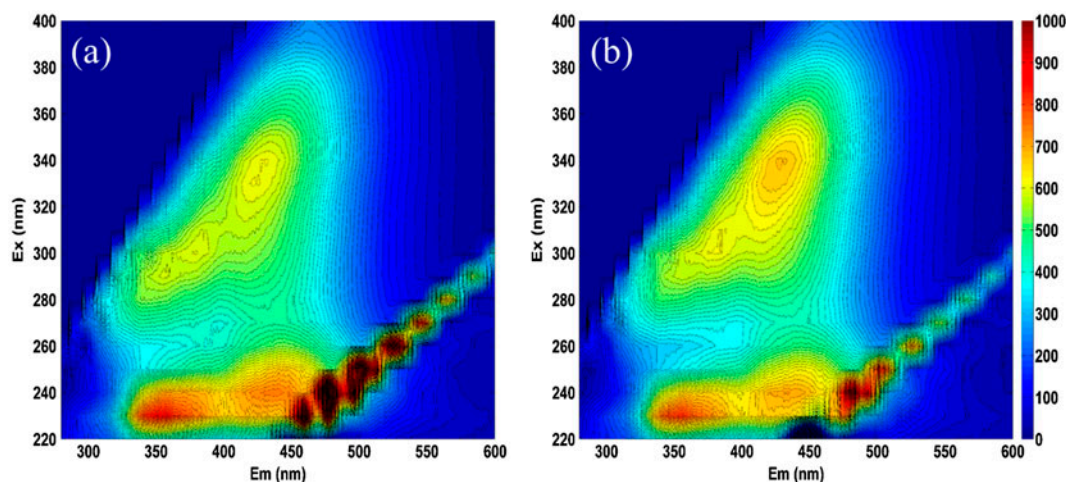
Fig. 4. FEEM images of concentrate made by pressure-driven filtration (at 20 bars) of (a) FOPA and (b) ROPA.
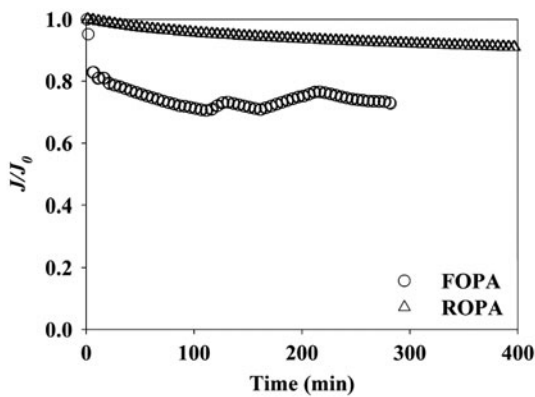
Fig. 5. Flux of pressure-driven filtration (J_0 was 102.53 for FOPA and 50.94 $Lm^{-2} h^{-1}$ for ROPA, respectively).

concentrations of 60 mg/L as DOC. The draw solution was 0.5 M NaCl and the water recovery was 50%. Fig. 6 illustrates fluorescence contour plots for the four solutions: The synthetic HA feed, the synthetic SA feed, concentrate from HA, and concentrate from SA solutions. The FO concentrates from the HA solution showed a much higher humic acid-like peak than the feed HA, indicating an effective rejection of humic acid by the FOPA membrane.

The water quality results also corresponded with the high intensity of HA, as shown in Table 4. The DOC and UVA of HA concentrates increased by concentration factors of 2.23–3.5, respectively. However, the intensity of the FO concentrate from the SA solution was similar to that of the feed SA, suggesting that the sodium alginate did not remain in the bulk solution. Sodium alginate is a polysaccharide and is a known organic fouling matter in membrane processes [10].

The flux decline patterns of two feed solutions during FO filtration are illustrated in Fig. 7. Flux decline occurred with both solutions, which was consistent with results from Lee et al. [11]. The authors of the paper used 200 mg/L of alginate, humic acid, and BSA to compare the fouling tendencies of FO and RO filtration. The FO flux by alginate and humic acid was substantially reduced compared to the RO flux, whereas the FO flux by BSA declined less than the RO flux. The authors described the significant flux decline of FO filtration as resulting from the greater cake-enhanced osmotic pressure (CEOP) and much thicker cake layers. In the FO process, a
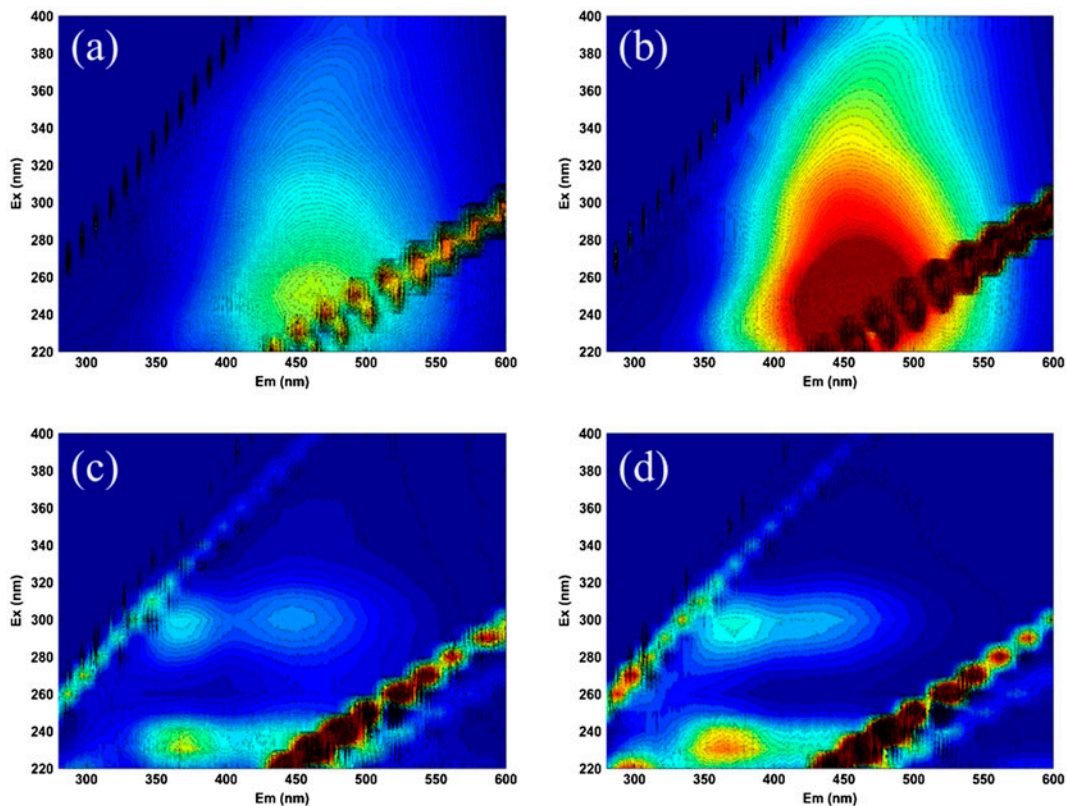
Fig. 6. FEEM images of concentrate from HA and SA filtered by FOPA of (a) HA (60 mg/L as DOC), (b) HA concentrate, (c) SA (60 mg/L as DOC), and (d) SA concentrate.

Table 4
Summary of water quality for HA and SA

	DOC (mg/L)	UV$_{254}$ (cm^{-1})	SUVA (L/m mg)
HA	61.23 ± 0.2	0.143	0.234
SA	65.35 ± 0.1	0.003	0.005
HA concentrate	136.63 ± 0.4	0.502	0.367
SA concentrate	85.23 ± 0.3	0.004	0.005
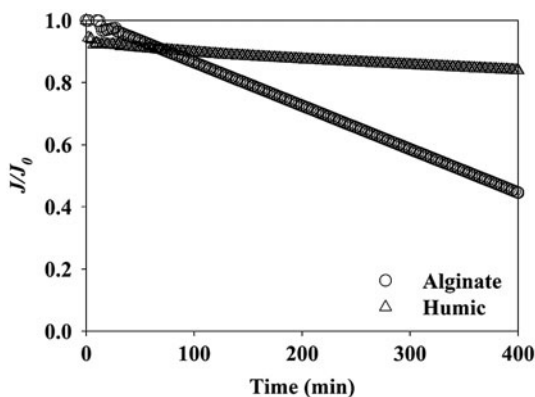
Fig. 7. Flux of HA and SA (J_0 was 10.23–12.58 Lm^{-2} m^{-1} for SA and HA, respectively).

high salt concentration in the draw side induces the reserve diffusion of salt to the feed side of the membrane, which is referred to as reverse salt flux (RSF). The RSF is known to significantly contribute to flux decline through accelerated CEOP. The salts diffused to the feed side were captured by the fouling layer [11]. The elevated concentrations of salt in the fouling layer yielded the great flux decline. In pressure-driven membrane processes, such as RO and NF, the presence of hydraulic pressure weakens the RSF and affects the fouling tendencies [11,19,20].

The degree of flux decline of the two solutions showed a significant difference. A more severe flux decline was observed with the SA solution than the HA solution. According to the water quality results and FEEM intensity contour plots, the low concentration of SA in the concentrate led to the belief that the SA had deposited and accumulated on the membrane surface, thus yielding a great amount of fouling. Particular hydrophilic organic matter, such as SA, might generate much greater organic fouling on the active layer of FOPA than hydrophobic organic matter such as HA [21].

4. Conclusions

Based on the results obtained in this study, the following conclusions can be drawn.

Fluorescence intensity using FEEM showed that organic matter in the SWE was effectively concentrated by the FO process. The intensity of the concentrate from FOPA illustrated a much higher humic acid-like peak C than that of the SWE. The concentrate from ROPA was dominated by the tryptophan protein-like peak A.

The MW distribution of DOM showed that the FO concentrate from FOPA contained 20% more nonbiodegradable organic matter such as humics and building blocks than the SWE.

Based on the results obtained in the pressure-driven filtration experiments, the presence of hydraulic pressure weakened the RSF and affected the fouling tendencies. Thus, the characteristics of the concentrates were very similar.

Natural organic matter is known as a critical fouling matter for membrane processes such as RO and NF. However, the generation of organic fouling on the surface of FOPA could differ due to the hydrophobicity of organic matter.

References

[1] O. Bakajin, E. Desormeaux, J. Klare, Opportunities and challenges in commercialization of forward osmosis membrane processes, in: 8th International Desalination Workshop (IDW) Session C: Keynote, Jeju, Korea, Nov 18–21, 2015, pp. 27–29.
[2] T.Y. Cath, D. Adams, A.E. Childress, Membrane contactor processes for wastewater reclamation in space: II. Combined direct osmosis, osmotic distillation, and membrane distillation for treatment of metabolic wastewater, J. Membr. Sci. 257(1–2) (2005) 111–119.

[3] T.Y. Cath, N.T. Hancock, C.D. Lundin, C. Hoppe-Jones, J.E. Drewes, A multi-barrier osmotic dilution process for simultaneous desalination and purification of impaired water, J. Membr. Sci. 362(1–2) (2010) 417–426.

[4] N.T. Hancock, P. Xu, M.J. Roby, J.D. Gomez, T.Y. Cath, Towards direct potable reuse with forward osmosis: Technical assessment of long-term process performance at the pilot scale, J. Membr. Sci. 445 (2013) 34–46.

[5] R.V. Linares, Z. Li, S. Sarp, S.S. Bucs, G. Amy, J.S. Vrouwenvelder, Forward osmosis niches in seawater desalination and wastewater reuse, Water Res. 66 (2014) 122–139.

[6] R.V. Linares, V. Yangali-Quintanilla, Z. Li, G. Amy, NOM and TEP fouling of a forward osmosis (FO) membrane: Foulant identification and cleaning, J. Membr. Sci. 421–422 (2012) 217–224.

[7] S.J. Khan, D. Murchland, M. Rhodes, T.D. Waite, Management of concentrated waste streams from high-pressure membrane water treatment systems, Crit. Rev. Env. Sci. Technol. 39(5) (2009) 367–415.

[8] V. Yangali-Quintanilla, Z. Li, R. Valladares, Q. Li, G. Amy, Indirect desalination of red sea water with forward osmosis and low pressure reverse osmosis for water reuse, Desalination 280(1–3) (2011) 160–166.

[9] R.V. Linares, V. Yangali-Quintanilla, Z. Li, G. Amy, Rejection of micropollutants by clean and fouled forward osmosis membrane, Water Res. 45(20) (2011) 6737–6744.

[10] J.W. Nam, S.H. Hong, J.Y. Park, H.S. Park, H.S. Kim, A. Jang, Evaluation of chemical cleaning efficiency of organic-fouled SWRO membrane by analyzing filtration resistance, Desalin. Water Treat. 51(31–33) (2013) 6172–6178.

[11] S. Lee, C. Boo, M. Elimelech, S. Hong, Comparison of fouling behavior in forward osmosis (FO) and reverse osmosis (RO), J. Membr. Sci. 365(1–2) (2010) 34–39.

[12] W. Chen, P. Westerhoff, J.A. Leenheer, K. Booksh, Fluorescence excitation—Emission matrix regional integration to quantify spectra for dissolved organic matter, Environ. Sci. Technol. 37(24) (2003) 5701–5710.

[13] S. Baghoth, M. Dignum, A. Grefte, J. Kroesbergen, G. Amy, Characterization of NOM in a drinking water treatment process train with no disinfectant residual, Water Sci. Technol. 9(4) (2009) 379–386.

[14] APHA, Standard Methods for the Examination of Water and Wastewater, twenty-first ed., 448 American Public Health Association/American Water Works Association/Water 449 Environment Federation, Washington DC, USA, 2005.

[15] N. Her, G. Amy, D. McKnight, J. Sohn, Y. Yoon, Characterization of DOM as a function of MW by fluorescence EEM and HPLC-SEC using UVA, DOC, and fluorescence detection, Water Res. 37(17) (2003) 4295–4303.

[16] T.F. Marhaba, R.L. Lippincott, Application of fluorescence technique for rapid identification of DOM fractions in source waters, J. Environ. Eng. 126(11) (2000) 1039–1044.

[17] S. Huber, F.H. Frimmel, A liquid chromatographic system with multi-detection for the direct analysis of hydrophilic organic compounds in natural waters, Fresenius´ J. Anal. Chem. 342(1–2) (1992) 198–200.

[18] N.Y. Yip, A. Tiraferri, W.A. Phillip, J.D. Schiffman, M. Elimelech, High performance thin-film composite forward osmosis membrane, Environ. Sci. Technol. 44 (10) (2010) 3812–3818.

[19] C. Boo, S. Lee, M. Elimelech, Z. Meng, S. Hong, Colloidal fouling in forward osmosis: Role of reverse salt diffusion, J. Membr. Sci. 390–391 (2012) 277–284.

[20] Y. Kim, M. Elimelech, H.K. Shon, S. Hong, Combined organic and colloidal fouling in forward osmosis: Fouling reversibility and the role of applied pressure, J. Membr. Sci. 460 (2014) 206–212.

[21] B. Mi, M. Elimelech, Organic fouling of forward osmosis membranes: Fouling reversibility and cleaning without chemical reagents, J. Membr. Sci. 348(1–2) (2010) 337–345.